

Reactivity of a Thiolate-Bridged Dinuclear Ruthenium Complex with Nitrogenous Molecules: Spectroscopic Identification of a Labile Dinitrogen Complex^[‡]

Dieter Sellmann,^{[a][†]} Raju Prakash,^{*,[a,b]} and Frank W. Heinemann^[a]

Dedicated to Prof. Dr. Joachim Sieler on the occasion of his 65th birthday

Keywords: N ligands / Nitrogenases / Nitrogen fixation / Ruthenium / S ligands

Reactions of the thiolate-bridged diruthenium complex $[\text{Ru}(\text{py}^{\text{bu}}\text{S}_4)]_2$ (**1**) ($\text{py}^{\text{bu}}\text{S}_4^{2-} = 2,6\text{-bis}[(3,5\text{-di-}i\text{-tert-butyl-2-sulfanylphenyl)thiomethyl}]pyridine(2-)]$) with small-molecule ligands *L* afforded the corresponding mononuclear complexes $[\text{Ru}(\text{L})(\text{py}^{\text{bu}}\text{S}_4)]$ [*L* = H^- (**2**); CH_3CN (**3**); NH_3 (**4**); CO (**5**); N_2H_4 (**6**); PMe_3 (**7**); N_3^- (**8**)]. The molecular structures of **3**, **4**, and **5** exhibit pseudooctahedral geometry with two thiolate and two thioether donor atoms in a *trans* configuration. Complexes **2–8** exhibit a quasi-reversible, one-electron redox wave of the $\text{Ru}^{\text{II}}/\text{Ru}^{\text{III}}$ couple in the region between $E_{1/2} = +0.214$ and $+0.460$ V vs. NHE. Complex **1** reacts reversibly with N_2 (60 bar) at 40°C to give the labile dinitrogen complex $[\text{Ru}(\text{N}_2)(\text{py}^{\text{bu}}\text{S}_4)]$ (**9**). Complex **9** can also be obtained from the reaction between **3** and N_2 (20 bar) at room

temperature. Treatment of **4** with NO afforded the labile 19-valence-electron species $[\text{Ru}(\text{NO})(\text{py}^{\text{bu}}\text{S}_4)]$ (**10**) in solution, which could subsequently be converted to **9** upon high-pressure reaction with N_2 (20 bar). In contrast, the analogous reaction of **4** with NOBF_4 results in the formation of the oxidized complex $[\text{Ru}(\text{NH}_3)(\text{py}^{\text{bu}}\text{S}_4)]\text{BF}_4$ (**11**), the structure of which was confirmed by X-ray structure analysis. The carbonyl complex $[\text{Ru}(\text{CO})(\text{py}^{\text{bu}}\text{S}_4)]$ (**5**) could be reversibly protonated at the thiolate sulfur atom to give $[\text{Ru}(\text{CO})(\text{py}^{\text{bu}}\text{S}_4\text{H})]\text{BF}_4$ (**12**). UV irradiation of **5** and **12** under N_2 at -80°C produced the short-lived species **9** and **13**, respectively, which were identified spectroscopically.

(© Wiley-VCH Verlag GmbH & Co. KGaA, 69451 Weinheim, Germany, 2004)

Introduction

Nitrogenases comprise sulfur-dominated polynuclear FeMo, FeV or FeFe cofactors as their active sites, which catalyze the transformation of dinitrogen to ammonia under mild conditions.^[1] Coordination of N_2 to a sulfur-rich transition metal complex is thought to be an effective strategy towards nitrogen fixation.^[2] Despite numerous intensive efforts,^[3] metal–sulfur complexes that bind molecular nitrogen are very scarce.^[4] However, it is believed that systematic in-depth studies on sulfur-rich transition metal complexes with biologically relevant molecules such as CO, NO,

N_2H_2 , N_2H_4 , N_3^- etc. will shed light on this intriguing N_2 activation and its exploitation to produce ammonia under mild conditions. As part of our contribution in this field, we recently obtained the mononuclear and dinuclear dinitrogen complexes $[\text{Ru}(\text{N}_2)(\text{PR}_3)(\text{N}_2\text{Me}_2\text{S}_2)]$ and $[\mu\text{-N}_2\{\text{Ru}(\text{PR}_3)(\text{N}_2\text{Me}_2\text{S}_2)\}_2]$ [*R* = *i*Pr, Cy; $\text{N}_2\text{Me}_2\text{S}_2^{2-} = N,N'$ -dimethyl-1,2-ethanediamine-*N,N'*-bis(benzenethiolate)-(2-)] by direct reaction of $[\text{Ru}(\text{CH}_3\text{CN})(\text{PR}_3)(\text{N}_2\text{Me}_2\text{S}_2)]$ with molecular nitrogen under very mild conditions.^[5] However, attempts to reduce the coordinated N_2 in these complexes were unsuccessful due to decoordination of the N_2 ligand. Meanwhile, we developed the fragment $[\text{M}(\text{pyS}_4)]$ (*M* = Fe, Ru or Os; $\text{pyS}_4^{2-} = 2,6\text{-bis}[(2\text{-sulfanylphenyl)thiomethyl}]pyridine(2-)]$, which readily binds a number of small nitrogenase-relevant ligands. The resultant six-coordinate mononuclear complexes are redox-active and are formed diastereoselectively by maintaining the thiolate and thioether donors always *trans* to each other.^[6] However, none of these metal fragments is capable of binding molecular nitrogen, even at elevated N_2 pressure (200 bar) and high temperature (100°C).

[‡] Transition Metal Complexes with Sulfur Ligands, 166. Part 165: D. Sellmann, K. Hein, F. W. Heinemann, *Inorg. Chim. Acta*, in press.

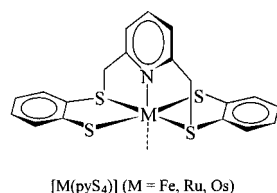
[†] Deceased.

[a] Institut für Anorganische Chemie der Universität Erlangen-Nürnberg, Egerlandstrasse 1, 91058 Erlangen, Germany

[b] Institut für Organische Chemie der Universität Erlangen-Nürnberg, Henkestrasse 42, 91054 Erlangen, Germany

Fax: 49-9131-852-1165

E-mail: raju.prakash@chemie.uni-erlangen.de



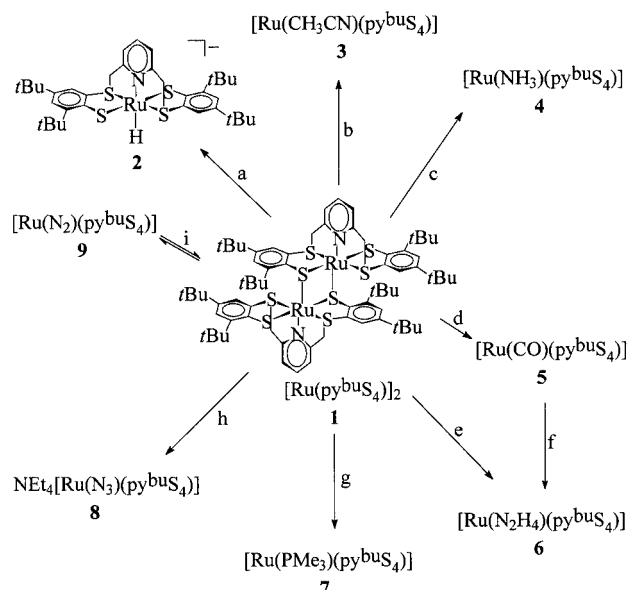
Recently, we achieved the heterolytic cleavage of H_2 at room temperature using the thiolate-bridged diruthenium complex $[\text{Ru}(\text{py}^{\text{bu}}\text{S}_4)]_2$ (**1**) $\{\text{py}^{\text{bu}}\text{S}_4^{2-} = 2,6\text{-bis}[(3,5\text{-di-}t\text{-butyl-2-sulfanylphenyl})\text{thiomethyl}]\text{pyridine}(2-)\}$ to form the hydride protonated thiolate $[\text{Ru}(\text{H})(\text{py}^{\text{bu}}\text{S}_4\text{H})]$.^[7] The latter species, in turn, reacts with a base to give the hydride $[\text{Ru}(\text{H})(\text{py}^{\text{bu}}\text{S}_4)]^-$ by abstraction of the S–H proton. This remarkable result prompted us to further investigate the reactivity of **1** towards nitrogenase-relevant molecules. Herein we describe the synthesis and characterization of the mononuclear complexes $[\text{Ru}(\text{L})(\text{py}^{\text{bu}}\text{S}_4)]$ ($\text{L} = \text{H}^-, \text{CO}, \text{NH}_3, \text{N}_2\text{H}_4, \text{CH}_3\text{CN}, \text{N}_3^-, \text{etc.}$) starting from complex **1**. The reaction of these complexes and of **1** with molecular nitrogen to form labile dinitrogen complexes is also reported.

Results and Discussion

Synthesis and Characterization of $[\text{Ru}(\text{L})(\text{py}^{\text{bu}}\text{S}_4)]$ Complexes

The preparation of ruthenium complexes $[\text{Ru}(\text{L})(\text{py}^{\text{bu}}\text{S}_4)]$ containing the σ or $\sigma\text{-}\pi$ ligands L is a prerequisite for probing the influence of L on the potential coordination of the N_2 ligand. Scheme 1 summarizes the syntheses of $[\text{Ru}(\text{L})(\text{py}^{\text{bu}}\text{S}_4)]$. The new complexes were prepared by the reaction of dinuclear complex **1** with nucleophiles L by the dissociation of the Ru–S bridges.

Treatment of complex **1** with a fivefold excess of NaAlH_4 in THF under argon yields extremely air- and moisture-sensitive $[\text{Na}[\text{Ru}(\text{H})(\text{py}^{\text{bu}}\text{S}_4)]]$ (**2**), which can be isolated in the solid state conveniently at room temperature, and is obtained with much better yield (65%) than that of our previous method.^[7] Refluxing of a suspension of **1** in CH_3CN continuously for 2 d affords $[\text{Ru}(\text{CH}_3\text{CN})(\text{py}^{\text{bu}}\text{S}_4)]$ (**3**). In the course of the reaction, the pink suspension of **1** changes to an orange solution, from which **3** could be obtained in a reasonable yield (48%). Treatment of **1** with NH_3 or CO in THF under normal conditions leads to the formation of $[\text{Ru}(\text{NH}_3)(\text{py}^{\text{bu}}\text{S}_4)]$ (**4**) or $[\text{Ru}(\text{CO})(\text{py}^{\text{bu}}\text{S}_4)]$ (**5**), respectively. In the former case, the pink suspension changes to a wine-red solution which exhibits the $\nu(\text{NH})$ bands in the IR (THF) spectrum in the region of $3350\text{--}3000\text{ cm}^{-1}$, whereas in the latter case the resulting yellow solution shows a strong carbonyl band at 1967 cm^{-1} . At 70°C , compound **1** reacts with a tenfold excess of N_2H_4 to afford $[\text{Ru}(\text{N}_2\text{H}_4)(\text{py}^{\text{bu}}\text{S}_4)]$ (**6**) in an isolated yield of 67%. Alternatively, UV irradiation of the 18-valence-electron carbonyl complex **5** in the presence of an excess of N_2H_4 in THF at -30°C proceeds efficiently with the extrusion of CO and subsequent coordination of the N_2H_4 molecule to afford **6**



Scheme 1. Synthesis of $[\text{Ru}(\text{L})(\text{py}^{\text{bu}}\text{S}_4)]$ complexes: (a) excess NaAlH_4 , -78 to 20°C , 2 h, THF; (b) CH_3CN , RF, 2 d; (c) excess NH_3 , 20 h, THF; (d) excess CO, 15 h, THF; (e) excess N_2H_4 , 70°C , 1 d, THF; (f) excess N_2H_4 , UV, -30°C , 1 h, THF; (g) PMe_3 , 2 h, THF; (h) excess NEt_4N_3 , 2 d, THF; (i) N_2 (60 bar), 40°C , 7 d, THF

(91%). In the course of the reaction, the yellow solution changes to red. The $\nu(\text{CO})$ band of **5** proved to be a good probe for monitoring the reaction by IR spectroscopy. The yellow-red complex $[\text{Ru}(\text{PMe}_3)(\text{py}^{\text{bu}}\text{S}_4)]$ (**7**) was formed instantaneously when a suspension of **1** in THF was treated with a slight excess of PMe_3 . The labile azido complex $\text{NEt}_4[\text{Ru}(\text{N}_3)(\text{py}^{\text{bu}}\text{S}_4)]$ (**8**) can be obtained only after 2 d by vigorous stirring of the THF suspension of **1** with an excess of NEt_4N_3 .

Most new complexes were isolated in analytically pure form, are soluble in THF, CH_2Cl_2 , acetone, DMF or DMSO, and were characterized by IR and NMR spectroscopy, mass spectrometry and/or X-ray crystallography. The IR (KBr) spectra of the complexes exhibit a typical absorption pattern for the $[\text{Ru}(\text{py}^{\text{bu}}\text{S}_4)]$ fragment. In addition, the spectrum of **3** exhibits a sharp band at 2269 cm^{-1} for the CN stretching vibration of the CH_3CN ligand. The NH_3 and N_2H_4 ligands of **4** and **6**, respectively, gave rise to sharp $\nu(\text{NH})$ bands in the region $3350\text{--}3000\text{ cm}^{-1}$, whereas the $\nu(\text{N}_3)$ band of **8** appears at 2022 cm^{-1} . As judged by their well-resolved NMR spectra, the complexes are diamagnetic. The ^1H NMR spectra of all complexes show a characteristic splitting pattern for the $[\text{Ru}(\text{py}^{\text{bu}}\text{S}_4)]$ fragment, consisting of three doublets and a multiplet for the aromatic protons, two doublets for the bridging CH_2 groups, and two singlets for the $t\text{Bu}$ groups. The number of ^1H and ^{13}C NMR signals for **2–8** (see Exp. Sect.) are consistent with a C_2 symmetry in solution, which has also been confirmed by the X-ray structure determinations of **3**, **4** and **5**. The cyclic voltammogram of **1** (Figure 1) shows two quasi-reversible one-electron waves at $E_{1/2} = +0.450$ and $+0.760\text{ V}$ for the $\text{Ru}^{\text{II,II}}/\text{Ru}^{\text{II,III}}$ and $\text{Ru}^{\text{II,III}}/$

$\text{Ru}^{\text{III,III}}$ redox couples, respectively. All mononuclear complexes exhibit the quasi-reversible redox wave of the $\text{Ru}^{\text{II}}/\text{Ru}^{\text{III}}$ couple in the region between $E_{1/2} = +0.214$ and $+0.460$ V.

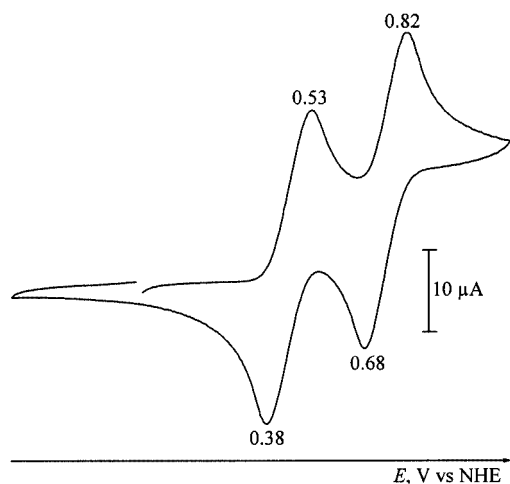


Figure 1. Cyclic voltammogram of **1** in THF (10^{-3} M; NBu_4PF_6 , 10^{-1} M; $v = 50 \text{ mV s}^{-1}$; $T = 25^\circ\text{C}$)

The molecular structures of $[\text{Ru}(\text{CH}_3\text{CN})(\text{py}^{\text{bu}}\text{S}_4)] \cdot 2\text{CH}_3\text{CN}$ (**3**· $2\text{CH}_3\text{CN}$), $[\text{Ru}(\text{NH}_3)(\text{py}^{\text{bu}}\text{S}_4)] \cdot \text{CH}_2\text{Cl}_2 \cdot 0.5n\text{-pentane}$ (**4**· $\text{CH}_2\text{Cl}_2 \cdot 0.5n\text{-pentane}$) and $[\text{Ru}(\text{CO})(\text{py}^{\text{bu}}\text{S}_4)] \cdot \text{CH}_3\text{OH} \cdot (\text{CH}_3)_2\text{CO}$ [**5**· $\text{CH}_3\text{OH} \cdot (\text{CH}_3)_2\text{CO}$] were determined by single-crystal X-ray structure analysis. Figure 2 depicts the molecular structures and Table 1 lists selected distances and angles.

The unit cells of **3–5** contain one or more solvent molecules. In each compound the ruthenium center (Ru1) is surrounded by one N, four S, and one X (X = C, N or P) atoms in a pseudooctahedral geometry. The thioether and thiolate donors are *trans* to each other, with the pyridine N donor in an apical position such that a square-pyramidal $[\text{RuNS}_4]$ core results for the $[\text{Ru}(\text{py}^{\text{bu}}\text{S}_4)]$ fragment. The sixth position, *trans* to the pyridine N donor, is occupied by the X atom of the co-ligand L. The distances (except Ru–N1) and angles around the ruthenium atom are in the range usually found for diamagnetic six-coordinate Ru^{II} thiolate complexes.^[8] The Ru–S(thiolate) distances (236–239 pm) are usually longer than the Ru–S(thioether) distances (229–231 pm). In particular, short distances are observed for Ru1–N1 *trans* to the coligands CH_3CN and NH_3 [203.3(6) pm in **3** and 203.6(3) in **4**]. These distances are distinctly shorter than the corresponding distance in **5** [212.1(6) pm], as well as those of $[\text{Ru}(\text{L})(\text{py}^{\text{bu}}\text{S}_4)]$ (L = NO, HNO; 210–213 pm)^[8,9] and $[\text{Ru}(\text{L})(\text{pyS}_4)]$ (L = CO, PPh_3 , DMSO; 209–212 pm),^[10] indicating that in **3** and **4** a practically identical *trans* effect is imposed by the CH_3CN and NH_3 ligands.

Reactions with Dinitrogen

Treatment of **1** with N_2 under normal conditions did not result in any reaction. However, at 60 bar and 40°C the

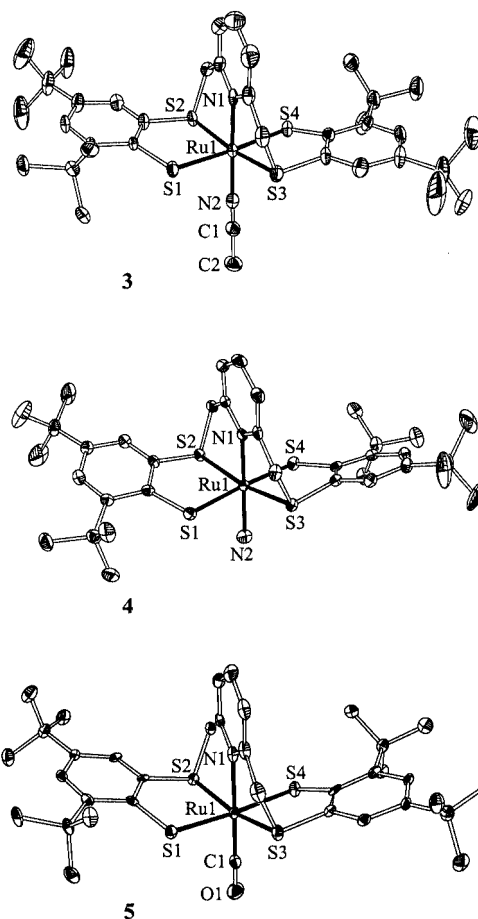


Figure 2. Thermal ellipsoid plots of $[\text{Ru}(\text{CH}_3\text{CN})(\text{py}^{\text{bu}}\text{S}_4)] \cdot 2\text{CH}_3\text{CN}$ (**3**· $2\text{CH}_3\text{CN}$), $[\text{Ru}(\text{NH}_3)(\text{py}^{\text{bu}}\text{S}_4)] \cdot \text{CH}_2\text{Cl}_2 \cdot 0.5n\text{-pentane}$ (**4**· $\text{CH}_2\text{Cl}_2 \cdot 0.5n\text{-pentane}$) and $[\text{Ru}(\text{CO})(\text{py}^{\text{bu}}\text{S}_4)] \cdot \text{CH}_3\text{OH} \cdot (\text{CH}_3)_2\text{CO}$ [**5**· $\text{CH}_3\text{OH} \cdot (\text{CH}_3)_2\text{CO}$] (50% probability ellipsoids; H atoms and solvent molecules omitted)

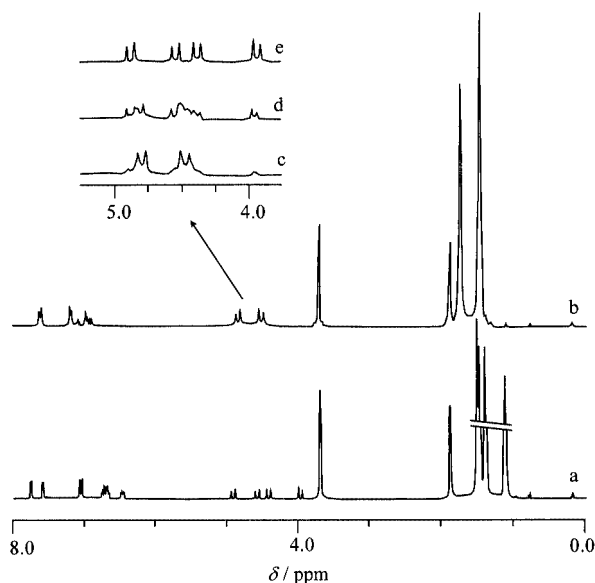
Table 1. Selected bond lengths [pm] and angles [$^\circ$] for $[\text{Ru}(\text{CH}_3\text{CN})(\text{py}^{\text{bu}}\text{S}_4)] \cdot 2\text{CH}_3\text{CN}$ (**3**· $2\text{CH}_3\text{CN}$), $[\text{Ru}(\text{NH}_3)(\text{py}^{\text{bu}}\text{S}_4)] \cdot \text{CH}_2\text{Cl}_2 \cdot 0.5n\text{-pentane}$ (**4**· $\text{CH}_2\text{Cl}_2 \cdot 0.5n\text{-pentane}$), $[\text{Ru}(\text{CO})(\text{py}^{\text{bu}}\text{S}_4)] \cdot \text{CH}_3\text{OH} \cdot (\text{CH}_3)_2\text{CO}$ [**5**· $\text{CH}_3\text{OH} \cdot (\text{CH}_3)_2\text{CO}$], $[\text{Ru}(\text{NH}_3)(\text{py}^{\text{bu}}\text{S}_4)]\text{BF}_4 \cdot \text{CD}_2\text{Cl}_2$ (**11**· CD_2Cl_2) and $[\text{Ru}(\text{NH}_3)(\text{py}^{\text{bu}}\text{S}_4\text{-O}_2)]\text{BF}_4 \cdot \text{CD}_2\text{Cl}_2$ (**11a**· CD_2Cl_2)

	3	4	5	11	11a
Ru1–N1	203.3(6)	203.6(3)	212.1(6)	206.3(3)	206.3(3)
Ru1–N2	202.5(6)	215.8(3)	185.1(7) ^[a]	214.1(4)	214.1(4)
Ru1–S1	238.6(2)	236.5(1)	237.8(2)	229.6(1)	229.6(1)
Ru1–S2	229.4(2)	228.8(1)	231.3(2)	231.8(2)	231.8(2)
Ru1–S3	229.5(2)	229.5(1)	231.2(2)	229.9(2)	229.9(2)
Ru1–S4	237.5(2)	236.5(1)	239.6(2)	231.8(1)	231.8(1)
S4–O41	—	—	—	—	157(1)
S4–O42	—	—	—	—	142(1)
N1–Ru1–N2	178.8(2)	178.9(2)	179.4(3) ^[a]	178.1(2)	178.1(2)
N1–Ru1–S1	88.2(2)	91.77(8)	88.2(2)	89.99(9)	89.99(9)
S1–Ru1–S4	176.60(7)	174.85(4)	174.43(7)	178.69(4)	178.69(4)
S1–Ru1–S2	86.85(6)	86.51(3)	88.68(5)	87.25(4)	87.25(4)
S2–Ru1–S3	169.67(7)	167.53(3)	164.86(8)	168.79(4)	168.79(4)

^[a] N2 = C1.

¹H NMR spectroscopic monitoring of the reaction of **1** in [D₈]THF (or CD₂Cl₂ or [D₈]toluene) with N₂ (60 bar) in an autoclave specially constructed for the NMR tubes corroborated the IR spectroscopic data. Figure 3 shows the ¹H NMR spectra of **1** in [D₈]THF before and after pressurizing with N₂. The ¹H NMR spectrum of **1** under normal N₂ pressure is typical for a complex having C₁ symmetry (Figure 3a). When the suspension was pressurized with N₂ (60 bar) and allowed to react at 40 °C for 7 d, the ¹H NMR spectrum of the resulting red solution, recorded immediately after the release of the pressure, showed resonances that are characteristic of the mononuclear [Ru(py^{bu}S₄)] fragment with C₂ symmetry (Figure 3b). The new resonances gradually disappeared and the spectrum of **1** reappeared over a period of 60 min when the solution was kept under N₂ (Figure 3c–e, only the CH₂ resonances are shown). ¹H NMR spectroscopic monitoring of the reaction

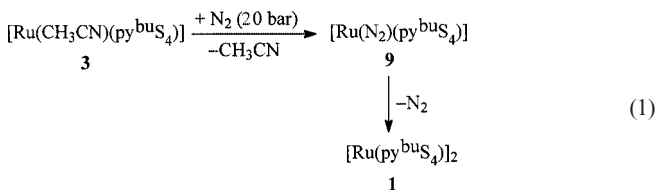
In another attempt, the substitution-labile acetonitrile complex **3** was treated with N₂. When N₂ was bubbled through a solution of **3** in THF for about 1 h, only **1** was formed, as indicated by the precipitation of pink-red microcrystals. The IR (THF) spectroscopic monitoring of the reaction inferred that the $\nu(\text{CN})$ band of **3** at 2269 cm⁻¹ is replaced by the $\nu(\text{CN})$ band of free CH₃CN at 2251 cm⁻¹. In contrast, the analogous reaction performed in an autoclave with N₂ (30 bar) at 20 °C for 2 d produced the labile species **9**. In the course of the reaction, the solution color changed from orange to red, and the IR (THF) spectrum exhibited two bands at 2251 and 2139 cm⁻¹ (Figure 4). The



Eur. J. Inorg. Chem. **2004**, 4291–4299

latter band, assigned to complex **9**, disappeared over the course of 1 h as the precipitate of **1** formed from the solution. The product isolated at $-80\text{ }^{\circ}\text{C}$ was found to be a mixture; however, it exhibits a weak, short-lived band in the IR (KBr) spectrum at 2134 cm^{-1} .

^1H NMR spectroscopic monitoring of the reaction of **3** in $[\text{D}_8]\text{THF}$ (or CD_2Cl_2) with N_2 (20 bar) in a pressure tube complements the earlier results. The ^1H NMR spectrum of **3** under N_2 shows the methyl resonance of CH_3CN at $\delta = 2.18\text{ ppm}$ (see Exp. Sect.). After pressurizing the NMR tube with N_2 (20 bar), the signal at $\delta = 2.18\text{ ppm}$ decreased as the resonance of free CH_3CN at $\delta = 1.93\text{ ppm}$ increased over the course of 6 h. Apart from this, new resonances whose chemical shifts are identical to those of the previous high-pressure experiment appeared. The resonance at $\delta = 2.18\text{ ppm}$ vanished and the intensities of the new resonances increased over the course of 2 d. These new resonances were, in turn, gradually replaced by the spectrum of **1** when the N_2 pressure was released, showing this conversion to be reversible. These findings can be interpreted as follows: the primary step is the nucleophilic substitution of the CH_3CN ligand by N_2 to give the intermediate species **9** showing the $\nu(\text{N}_2)$ band at 2139 cm^{-1} . At normal pressure, compound **9** rapidly loses its N_2 ligand with subsequent formation of the stable compound **1** [Equation (1)].



There are reports in the literature that the formation of dinitrogen complexes occurs in the reaction of NO with metal-bound ammonia.^[12] Isotopic-tracer and kinetic studies imply that the mechanism involves attack of NO at metal-bound ammonia and subsequent dehydration.^[13] Reaction of **4** with NO in THF yielded the 19-valence-electron neutral complex $[\text{Ru}(\text{NO})(\text{py}^{\text{bu}}\text{S}_4)]$ (**10**; IR: $\tilde{\nu} = 1640\text{ cm}^{-1}$) as the major product; some traces of 18-valence-electron cationic $[\text{Ru}(\text{NO})(\text{py}^{\text{bu}}\text{S}_4)]^+$ (IR: $\tilde{\nu} = 1886\text{ cm}^{-1}$) and N_2O (IR: $\tilde{\nu} = 2224\text{ cm}^{-1}$) were also found in solution. The solution of **10** is stable only under NO. Treatment of a solution of **10** with N_2 (50 bar) for 5 d caused the color of the solution to change from green to red; the resulting solution showed a weak band at 2139 cm^{-1} in the IR spectrum, indicating the formation of the N_2 species **9** in solution [Equation (2)]. In contrast to this, the analogous reaction of **4** with an equimolar amount of NOBF_4 resulted in the formation of the ruthenium(III) complex $[\text{Ru}(\text{NH}_3)(\text{py}^{\text{bu}}\text{S}_4)]\text{BF}_4$ (**11**), according to Equation (3). Figure 5 depicts the molecular structures of **11** and **11a**, and Table 1 lists selected bond lengths and angles.

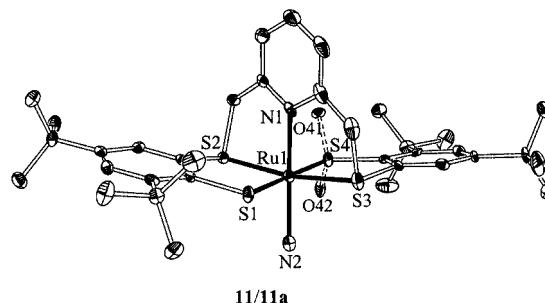
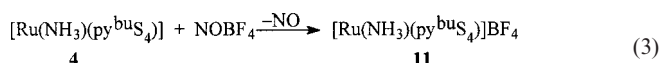
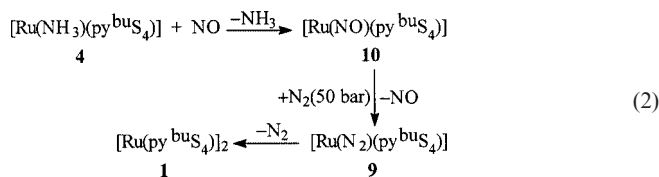


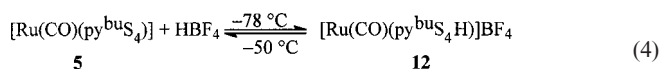
Figure 5. Thermal ellipsoid plots of $[\text{Ru}(\text{NH}_3)(\text{py}^{\text{bu}}\text{S}_4)]\text{BF}_4 \cdot \text{CD}_2\text{Cl}_2$ (**11**· CD_2Cl_2) (without S–O bonds) and $[\text{Ru}(\text{NH}_3)(\text{py}^{\text{bu}}\text{S}_4\text{O}_2)]\text{BF}_4 \cdot \text{CD}_2\text{Cl}_2$ (**11a**· CD_2Cl_2) (with S–O bonds) (50% probability ellipsoids; BF_4 counterion, H atoms and solvent molecules omitted)

The unit cell of **11** contains one molecule of CD_2Cl_2 per formula unit. The ruthenium(III) center is surrounded by two N and four S atoms in a pseudooctahedral geometry. The two thioether and two thiolate donors adopt *trans* positions, and the NH_3 ligand occupies the position *trans* to the pyridine N donor. The Ru–S(thiolate) and Ru–S(thioether) distances all lie in the range between 229 and 232 pm. This is in contrast to the corresponding distances of **4** as well as other $[\text{Ru}^{\text{II}}(\text{L})(\text{py}^{\text{bu}}\text{S}_4)]$ complexes, where the Ru–S(thiolate) distances are usually longer than the Ru–S(thioether) distances.^[8] The Ru–N(pyridine) distance in **11** is longer (by about 3 pm) than that of **4**. During crystallization of **11** complex **11a** is formed by aerial oxidation of **11**.

UV irradiation of complex **5** in CH_2Cl_2 while bubbling N_2 through the solution always yielded **1** as the final product. However, IR monitoring of this reaction suggested the formation of the intermediate species **9** in solution. The IR spectrum of the solution of **5** in CH_2Cl_2 shows the $\nu(\text{CO})$ band at 1967 cm^{-1} . Irradiation of this solution at $-80\text{ }^{\circ}\text{C}$ for 10 min gave rise to a new weak band at 2138 cm^{-1} , and subsequently the intensity of the $\nu(\text{CO})$ band decreased. On continuous irradiation, the intensity of both the bands decreased, and after 50 min microcrystals of **1** had precipitated.

Protonation of **5** with HBF_4 at $-80\text{ }^{\circ}\text{C}$ afforded the carbonyl protonated thiolate complex $[\text{Ru}(\text{CO})(\text{py}^{\text{bu}}\text{S}_4\text{H})]\text{BF}_4$ (**12**) according to Equation (4). The IR spectrum of **12** in CH_2Cl_2 exhibits the $\nu(\text{CO})$ band at 2001 cm^{-1} and the

$\nu(\text{SH})$ band at 2486 cm^{-1} . The CO absorption of **12** is red-shifted by about 34 cm^{-1} compared to that in **5**, which is in good agreement with values reported for the protonation of thiolate groups.^[6] Irradiation of **12**, analogous to **5**, initially gave rise to a band at 2172 cm^{-1} , which disappeared on further irradiation to give only an uncharacterizable red-brown solid. It is interesting to note that the difference in wavenumbers between the $\nu(\text{CO})$ and $\nu(\text{N}_2)$ bands in the corresponding complex pairs of **5** and **12** are 168 and 169 cm^{-1} , respectively. These values are in good agreement with those reported for other CO and N_2 complexes.^[3] Moreover, the frequency difference between the new bands formed during UV irradiation of **5** and **12** is 34 cm^{-1} for both complexes. These results indicate that the irradiation reactions of **5** and **12** in the presence of N_2 proceed by similar pathways; the first step may be the formation of the labile intermediate species $[\text{Ru}(\text{N}_2)(\text{py}^{\text{bu}}\text{S}_4)]$ (**9**) and $[\text{Ru}(\text{N}_2)(\text{py}^{\text{bu}}\text{S}_4\text{H})]\text{BF}_4$ (**13**), respectively. These species may either be subjected to irradiation or undergo simple decomplexation of the N_2 ligand to give the stable thiolate-bridged dimer or other products.



Taken together, these results demonstrate that the dinuclear complex **1** and the mononuclear complexes **3**, **5**, **10** and **12** are capable of coordinating molecular nitrogen under moderate pressures of N_2 to form the corresponding labile dinitrogen complexes, although attempts to isolate these species inevitably yielded only the more stable thiolate-bridged complex. Therefore, in an effort to stabilize the labile N_2 species, as well as to prevent the formation of Ru–S bridges, synthesis of a metal fragment containing electron-rich and sterically bulky substituent groups is in progress.

Conclusion

In the quest for transition metal–sulfur complexes that enable the modelling of the reactivity features and key intermediates of nitrogenases reactions, $[\text{Ru}(\text{L})(\text{py}^{\text{bu}}\text{S}_4)]$ complexes were synthesized and completely characterized. The molecular structures of **3**, **4** and **5** were determined by X-ray structure analysis. All complexes exhibit a pseudooctahedral geometry. The central metal atom is surrounded by at least two thiolate and two thioether groups in mutual *trans* positions, and has a well-approximated C_2 symmetry. The reactivity of $[\text{Ru}(\text{py}^{\text{bu}}\text{S}_4)]_2$ and $[\text{Ru}(\text{L})(\text{py}^{\text{bu}}\text{S}_4)]$ complexes towards molecular nitrogen was investigated. IR and NMR spectroscopic evidence for the formation of the labile mononuclear dinitrogen complexes has been found in the reactions between **1**, **3**, **5**, **10** or **12** and N_2 . The reaction of **4** with NO results in the formation of the labile 19-valence-electron NO complex **10**, while treatment of **4** with NOBF_4

yielded only the (ammonia)ruthenium(III) complex **11**. Attempts to isolate compound **9** were unsuccessful.

Experimental Section

General: All reactions and manipulations were carried out under Ar or N_2 using standard Schlenk techniques. Solvents were freshly dried with appropriate drying agents and distilled before use. Most reactions were monitored by IR or NMR spectroscopy. Physical measurements were carried out with the following instruments: IR (KBr discs or CaF_2 cuvettes, solvent bands were compensated), Perkin–Elmer 983, 1620 FT-IR and 16PC FT-IR; NMR: Jeol JNM-GX 270, Jeol JNM-EX 270, and Lambda LA 400 with the residual signals of the deuterated solvent used as an internal reference, chemical shifts are quoted in the δ scale (downfield shifts are positive); MS: Jeol MSTATION 700 spectrometer; elemental analysis: Carlo Erba EA 1106 or 1108 analyzer; cyclic voltammetry (CV): EG&G potentiostat PAR model 264A and a conventional three-electrode assembly consisting of a glassy-carbon working electrode and Pt reference and counter electrodes, solutions: THF (10^{-3} M), supporting electrolyte: NBu_4PF_6 (10^{-1} M), internal standard: ferrocene with $E(\text{F}_c/\text{F}_c^+) = +0.4\text{ V}$ vs. NHE,^[14] scan speed: 50 mV s^{-1} , $T = 25\text{ }^\circ\text{C}$, the reversibility of the voltammograms and the number of electrons involved in the redox processes were determined as described in the literature.^[15] NaAlH_4 (1 M solution in THF), N_2H_4 (1 M solution in THF) and NET_4N_3 were purchased from either Aldrich or Fluka. The compounds $[\text{Ru}(\text{NO})(\text{py}^{\text{bu}}\text{S}_4)]\text{Br}$ and $[\text{Ru}(\text{py}^{\text{bu}}\text{S}_4)]_2$ (**1**) were prepared as described in the literature.^[7,8b]

$\text{Na}[\text{Ru}(\text{H})(\text{py}^{\text{bu}}\text{S}_4)]$ (2**):** An excess of NaAlH_4 (4 mL, 1 M solution in THF, 4 mmol) was added to a pink-red suspension of **1** (500 mg, 0.35 mmol) in THF (20 mL) at $-80\text{ }^\circ\text{C}$. Upon warming, the suspension changed to a red solution. The solution was stirred at $20\text{ }^\circ\text{C}$ for 1 h, then the solvent was removed in vacuo. The resulting red residue was dissolved again in Et_2O (20 mL) and the insoluble colorless materials were removed by filtration. **Caution:** The colorless precipitate is extremely pyrophoric and should be handled with care! The filtrate was concentrated and treated with pentane to give red microcrystals of **2**. Yield: 336 mg (65%). $^1\text{H NMR}$ (269.7 MHz, $[\text{D}_8]\text{THF}$): $\delta = -14.85$ (s, 1 H, RuH), 1.28 (s, 18 H, *t*Bu), 1.51 (s, 18 H, *t*Bu), 4.42 (d, $^2J_{\text{H,H}} = 15.3\text{ Hz}$, 2 H, CH_2), 4.65 (d, $^2J_{\text{H,H}} = 15.3\text{ Hz}$, 2 H, CH_2), 6.90–6.83 (m, 3 H, $\text{C}_5\text{H}_3\text{N}$), 6.99 (d, $^3J_{\text{H,H}} = 1.9\text{ Hz}$, 2 H, C_6H_2), 7.51 (d, $^3J_{\text{H,H}} = 1.9\text{ Hz}$, 2 H, C_6H_2) ppm. $^{13}\text{C}\{^1\text{H}\}$ NMR (67.8 MHz, $[\text{D}_8]\text{THF}$): $\delta = 30.0$, 32.0, 34.8, 38.4 (*t*Bu), 62.4 (CH_2), 119.1, 122.5, 127.2, 129.7, 137.7, 142.2, 148.9, 154.9, 155.7 ($\text{C}_6\text{H}_2/\text{C}_5\text{H}_3\text{N}$) ppm. CV (vs. NHE): $E = +0.235\text{ V}$ ($\text{Ru}^{\text{II}}/\text{Ru}^{\text{III}}$).

$[\text{Ru}(\text{CH}_3\text{CN})(\text{py}^{\text{bu}}\text{S}_4)]$ (3**):** A suspension of **1** (500 mg, 0.35 mmol) in CH_3CN (25 mL) was refluxed for 2 d. The resulting orange-red solution was filtered, concentrated (2 mL), and treated with pentane to give orange microcrystals of **3**. Yield: 254 mg (48%). $\text{C}_{37}\text{H}_{52}\text{N}_2\text{ORuS}_4$ (770.17): calcd. C 57.70, H 6.80, N 3.63, S 16.65; found C 57.87, H 7.14, N 3.80, S 16.18. IR (KBr): $\tilde{\nu} = 2269\text{ cm}^{-1}$ $\nu(\text{CN})$. $^1\text{H NMR}$ (269.7 MHz, CD_3CN): $\delta = 1.31$ (s, 18 H, *t*Bu), 1.54 (s, 18 H, *t*Bu), 2.18 (s, 3 H, CH_3CN), 4.53 (d, $^2J_{\text{H,H}} = 16.1\text{ Hz}$, 2 H, CH_2), 4.68 (d, $^2J_{\text{H,H}} = 16.2\text{ Hz}$, 2 H, CH_2), 6.93 (d, $^3J_{\text{H,H}} = 7.7\text{ Hz}$, 2 H, $\text{C}_5\text{H}_3\text{N}$), 7.08 (t, $^3J_{\text{H,H}} = 2.0\text{ Hz}$, 1 H, $\text{C}_5\text{H}_3\text{N}$), 7.18 (d, $^3J_{\text{H,H}} = 2.1\text{ Hz}$, 2 H, C_6H_2), 7.58 (d, $^3J_{\text{H,H}} = 2.1\text{ Hz}$, 2 H, C_6H_2) ppm. $^{13}\text{C}\{^1\text{H}\}$ NMR (67.8 MHz, CD_3CN): $\delta = 22.5$ (CH_3CN), 29.6, 31.6, 34.9, 38.2 (*t*Bu), 57.5 (CH_2), 121.0, (C_6H_2), 124.3 (CH_3CN), 124.8, 127.9, 133.3, 134.4, 144.8, 149.2, 153.3,

160.0 (C₆H₂/C₅H₃N) ppm. FD-MS (CH₃CN): *m/z* = 752 [3⁺], 1422 [1⁺]. CV (vs. NHE): *E* = +0.214 V (Ru^{II}/Ru^{III}).

[Ru(NH₃)(py^{bu}S₄)] (4): NH₃ gas was bubbled through the suspension of **1** (300 mg, 0.21 mmol) in THF (10 mL) for 15 min, and the mixture was then stirred under NH₃ for 20 h. The resulting solution was concentrated (2 mL) and treated with pentane to give red microcrystals of **4**. Yield: 278 mg (92%). C₃₅H₅₀N₂RuS₄ (728.13): calcd. C 57.74, H 6.92, N 3.85, S 17.62; found C 57.76, H 6.87, N 3.94, S 17.38. IR (KBr): $\tilde{\nu}$ = 3344, 3262, 3175, 3084 cm⁻¹ ν(NH₃). ¹H NMR (269.7 MHz, [D₈]THF): δ = 1.30 (s, 18 H, *t*Bu), 1.59 (s, 18 H, *t*Bu), 1.71 (s, 3 H, NH₃), 4.45 (d, ²*J*_{H,H} = 15.5 Hz, 2 H, CH₂), 4.65 (d, ²*J*_{H,H} = 15.7 Hz, 2 H, CH₂), 6.95–6.80 (m, 3 H, C₅H₃N), 7.11 (d, ³*J*_{H,H} = 1.7 Hz, 2 H, C₆H₂), 7.55 (d, ³*J*_{H,H} = 1.8 Hz, 2 H, C₆H₂) ppm. ¹³C{¹H} NMR (67.8 MHz, [D₈]THF): δ = 30.0, 31.9, 34.8, 38.4 (*t*Bu), 57.8 (CH₂), 119.9, 123.6, 127.3, 130.3, 135.2, 143.4, 149.1, 154.2, 159.7 (C₆H₂/C₅H₃N) ppm. FD-MS (THF): *m/z* = 728 [4⁺], 1422 [1⁺]. CV (vs. NHE): *E* = +0.252 V (Ru^{II}/Ru^{III}).

[Ru(CO)(py^{bu}S₄)] (5): CO gas was bubbled through the suspension of **1** (350 mg, 0.24 mmol) in THF (10 mL) for 30 min, and the mixture was then stirred under CO for 15 h. The resulting yellow solution was filtered, concentrated (2 mL), and treated with Et₂O to give yellow microcrystals of **5**. Yield: 337 mg (94%). C₃₆H₄₇NORuS₄ (739.11): calcd. C 53.93, H 5.99, N 1.70, S 15.56; found C 54.13, H 5.95, N 1.69, S 15.38. IR (KBr): $\tilde{\nu}$ = 1967 cm⁻¹ ν(CO). ¹H NMR (269.7 MHz, [D₆]acetone): δ = 1.29 (s, 18 H, *t*Bu), 1.51 (s, 18 H, *t*Bu), 4.65 (d, ²*J*_{H,H} = 16.2 Hz, 2 H, CH₂), 4.95 (d, ²*J*_{H,H} = 16.3 Hz, 2 H, CH₂), 7.25 (d, ³*J*_{H,H} = 2.0 Hz, 2 H, C₆H₂), 7.36 (d, ³*J*_{H,H} = 7.7 Hz, 2 H, C₅H₃N), 7.53 (m, 1 H, C₅H₃N), 7.65 (d, ³*J*_{H,H} = 2.0 Hz, 2 H, C₆H₂) ppm. ¹³C{¹H} NMR (67.8 MHz, [D₆]acetone): δ = 29.9, 31.7, 35.0, 38.3 (*t*Bu), 59.2 (CH₂), 121.9, 125.0, 127.7, 133.9, 136.9, 145.5, 149.8, 151.9, 156.9 (C₆H₂/C₅H₃N), 202.8 (CO) ppm. FD-MS (THF): *m/z* = 739 [5⁺]. CV (vs. NHE): *E* = +0.458 V (Ru^{II}/Ru^{III}).

[Ru(N₂H₄)(py^{bu}S₄)] (6): (a): N₂H₄ (3.5 mL, 1 M solution in THF, 3.5 mmol) was added to a suspension of **1** (250 mg, 0.17 mmol) in THF (15 mL), and was refluxed for 24 h. The red solution that resulted was filtered, reduced in volume and treated with pentane to give red microcrystals of **6**. Yield: 172 mg (67%). **(b):** A solution of **5** (300 mg, 0.21 mmol) and N₂H₄ (2 mL, 1 M solution in THF, 2 mmol) in THF (35 mL) was irradiated in a quartz immersion lamp apparatus with an Hg lamp (150 W) at –30 °C for 1 h. The resulting solution was filtered, reduced in volume and the product precipitated with pentane to give **6** as a red powder. Yield: 280 mg (91%). C₃₅H₅₁N₃RuS₄ (743.15): calcd. C 56.57, H 6.92, N 5.65, S 17.26; found C 56.59, H 7.14, N 5.38, S 17.08. IR (KBr): $\tilde{\nu}$ = 3334, 3202, 3101 cm⁻¹ ν(NH). ¹H NMR (269.7 MHz, CD₂Cl₂): δ = 1.32 (s, 18 H, *t*Bu), 1.59 (s, 18 H, *t*Bu), 3.45 (b, 2 H, NH₂NH₂), 4.15 (m, 2 H, NH₂NH₂), 4.42 (d, ²*J*_{H,H} = 15.8 Hz, 2 H, CH₂), 4.69 (d, ²*J*_{H,H} = 16.0 Hz, 2 H, CH₂), 6.89 (d, ³*J*_{H,H} = 7.6 Hz, 2 H, C₅H₃N), 6.94 (t, ³*J*_{H,H} = 7.5 Hz, 1 H, C₅H₃N), 7.21 (d, ³*J*_{H,H} = 2.0 Hz, 2 H, C₆H₂), 7.58 (d, ³*J*_{H,H} = 2.0 Hz, 2 H, C₆H₂) ppm. ¹³C{¹H} NMR (67.8 MHz, CD₂Cl₂): δ = 29.5, 31.6, 34.6, 38.0 (*t*Bu), 57.0 (CH₂), 120.0, 124.2, 127.2, 130.8, 134.0, 144.6, 149.3, 151.6, 158.9 (C₆H₂/C₅H₃N) ppm. FD-MS (THF): *m/z* = 743 [6⁺], 1422 [1⁺]. CV (vs. NHE): *E* = +0.284 V (Ru^{II}/Ru^{III}).

[Ru(PMe₃)(py^{bu}S₄)] (7): PMe₃ (52 mg, 0.68 mmol) was added to a suspension of **1** (250 mg, 0.17 mmol) in THF (10 mL) and stirred for 2 h. The resulting solution was filtered, reduced in volume and treated with pentane to give yellow-red microcrystals of **7**. Yield: 194 mg (71%). C₃₈H₅₆NPRuS₄ (787.181): calcd. C 57.98, H 7.17,

N 1.78, S 16.29; found C 57.74, H 7.08, N 1.64, S 16.08. ¹H NMR (269.7 MHz, [D₈]THF): δ = 1.06 (s, 9 H, PMe₃), 1.28 (s, 18 H, *t*Bu), 1.56 (s, 18 H, *t*Bu), 4.41 (d, ²*J*_{H,H} = 15.7 Hz, 2 H, CH₂), 4.62 (d, ²*J*_{H,H} = 15.8 Hz, 2 H, CH₂), 6.90–6.75 (m, 3 H, C₅H₃N), 7.09 (d, ³*J*_{H,H} = 1.7 Hz, 2 H, C₆H₂), 7.52 (d, ³*J*_{H,H} = 1.8 Hz, 2 H, C₆H₂) ppm. ¹³C{¹H} NMR (67.8 MHz, [D₈]THF): δ = 15.4 (PMe₃), 29.5, 31.3, 34.1, 38.2 (*t*Bu), 57.4 (CH₂), 119.4, 122.6, 127.1, 130.0, 134.7, 142.8, 148.3, 153.4, 158.7 (C₆H₂/C₅H₃N) ppm. ³¹P{¹H} NMR (161.8 MHz, [D₈]THF): δ = 18.6 (PMe₃) ppm. FD-MS (THF): *m/z* = 787 [4⁺]. CV (vs. NHE): *E* = +0.243 V (Ru^{II}/Ru^{III}).

Et₄N[Ru(N₃)(py^{bu}S₄)] (8): NEt₄N₃ (100 mg, 0.58 mmol) was added to a suspension of **1** (200 mg, 0.14 mmol) in THF (10 mL) and stirred for 2 d. The resulting solution was filtered, concentrated, and treated with pentane to give pink-red microcrystals of **8**. Yield: 115 mg (47%). IR (KBr): $\tilde{\nu}$ = 2022 cm⁻¹ ν(N₃). ¹H NMR (269.7 MHz, CD₃OD): δ = 0.50 (t, ³*J*_{H,H} = 7.3 Hz, 12 H, NEt₄), 1.28 (m, 8 H, NEt₄), 1.34 (s, 18 H, *t*Bu), 1.60 (s, 18 H, *t*Bu), 4.47 (d, ²*J*_{H,H} = 15.7 Hz, 2 H, CH₂), 4.68 (d, ²*J*_{H,H} = 15.8 Hz, 2 H, CH₂), 6.90–6.75 (m, 3 H, C₅H₃N), 7.13 (d, ³*J*_{H,H} = 1.7 Hz, 2 H, C₆H₂), 7.56 (d, ³*J*_{H,H} = 1.8 Hz, 2 H, C₆H₂) ppm. ¹³C{¹H} NMR (67.8 MHz, CD₃OD): δ = 8.2 (NEt₄), 29.5, 31.6, 34.6, 38.0 (*t*Bu), 52.4 (NEt₄), 56.6 (CH₂), 119.8, 124.5, 126.4, 130.8, 134.2, 146.6, 148.0, 151.8, 157.9 (C₆H₂/C₅H₃N) ppm. CV (vs. NHE): *E* = +0.293 V (Ru^{II}/Ru^{III}).

[Ru(NO)(py^{bu}S₄)] (10): NO gas was bubbled through a solution of **4** (300 mg, 0.41 mmol) in THF (15 mL) for 3 min. The resulting green solution was filtered under NO. IR (THF): $\tilde{\nu}$ = 1640 cm⁻¹ ν(NO).

[Ru(NH₃)(py^{bu}S₄)]BF₄ (11): NOBF₄ (35 mg, 0.30 mmol) was added to a solution of **4** (210 mg, 0.29 mmol) in THF (15 mL). The color of the solution changed instantaneously from red to green. K₂CO₃ (20.7 mg, 0.15 mmol) was added to this solution and stirred for 1 h. The solution was filtered, concentrated (2 mL) and treated with pentane to give green microcrystals of **10**. Yield: 202 mg (86%). C₃₅H₅₀BF₄N₂RuS₄ (814.94): calcd. C 51.59, H 6.18, N 3.44, S 15.74; found C 51.62, H 6.20, N 3.45, S 15.68. IR (KBr): $\tilde{\nu}$ = 3358, 3268, 3186, 3089 cm⁻¹ ν(NH₃). FD-MS (THF): *m/z* = 728 [Ru(NH₃)(py^{bu}S₄)⁺], 1422 [1⁺].

[Ru(CO)(py^{bu}S₄H)]BF₄ (12): HBF₄ (0.30 mL, 0.22 mmol) was added to a solution of **5** (300 mg, 0.21 mmol) in CH₂Cl₂ (10 mL) at –80 °C. The color of the solution changed from red-yellow to dark-green. IR (CH₂Cl₂): $\tilde{\nu}$ = 2001 cm⁻¹ ν(CO), 2486 cm⁻¹ ν(SH).

High-Pressure NMR Experiment in an Autoclave: In a special autoclave, an NMR tube containing a suspension of **1** (70 mg) in [D₈]THF (0.6 mL) was pressurized with N₂ (5.0 grade, 60 bar), and was kept at 40 °C for 7 d. The autoclave was cooled to room temperature, and the pressure was released. The resulting red solution was monitored by recording ¹H NMR spectra at various time intervals.

High-Pressure NMR Experiment: In a pressure NMR tube (524-PV-1, Wilmad, USA), a solution of **3** (50 mg) in [D₈]THF (0.6 mL) was pressurized with N₂ (5.0 grade, 20 bar). The reaction was monitored by recording ¹H NMR spectra at various time intervals for 2 d.^[7,16]

High-Pressure Autoclave Experiment. (a): In an autoclave, a tube containing a suspension of **1** (350 mg) in THF (15 mL) was pressurized with N₂ gas (60 bar), and the suspension was stirred at 40 °C for 4 d. The autoclave was cooled to –80 °C and the pressure was released. IR (THF) spectra were recorded of the red solution at

various time intervals. **(b):** In an autoclave, a tube containing an orange solution of **3** (200 mg) in THF (15 mL) was pressurized with N₂ gas (20 bar) and the solution was stirred at 20 °C for 2 d. The pressure was then released and IR (THF) spectra were recorded of the resulting red solution at various time intervals. **(c):** The pressure reaction was performed as in (b). The autoclave was frozen with liquid nitrogen and then the pressure was released. The temperature was raised to −80 °C, the red solution was filtered, and treated with cold pentane to give a red solid. IR (KBr): $\tilde{\nu}$ = 2134 cm^{−1} ν (N₂).

UV-Irradiation Reaction: At −80 °C and with vigorous N₂ bubbling, a solution of **5** (250 mg) or **12** (300 mg) in CH₂Cl₂ (35 mL) was irradiated in a quartz immersion lamp apparatus with an Hg lamp (150 W) for 1 h. The reaction was monitored by recording IR (CH₂Cl₂) spectra until a pink-red or brown precipitate had formed from the solution.

X-ray Structure Determination of [Ru(CH₃CN)(py^{bu}S₄)]·2CH₃CN (3·2CH₃CN), [Ru(NH₃(py^{bu}S₄)]·CH₂Cl₂·0.5*n*-pentane (4·CH₂Cl₂·0.5*n*-pentane), [Ru(CO)(py^{bu}S₄)]·CH₃OH·(CH₃)₂CO [5·CH₃OH·(CH₃)₂CO], [Ru(NH₃(py^{bu}S₄)]BF₄·CD₂Cl₂ (11·CD₂Cl₂) and [Ru(NH₃(py^{bu}S₄-O₂)]BF₄·CD₂Cl₂ (11a·CD₂Cl₂): Over the course of 5 d, red plates of 3·2CH₃CN crystallized from a saturated solution of **3** in CH₃CN at −25 °C. Red fragments of 4·CH₂Cl₂·0.5*n*-pentane were grown from a concentrated CH₂Cl₂ solution of **4** layered with pentane at 4 °C over 2 d. Red crystals of 4·0.5*n*-pentane were also formed from a solution of **4** in a THF/*n*-pentane mixture. Yellow plates of 5·CH₃OH·(CH₃)₂CO crystallized from a solution of **5** in acetone layered with CH₃OH at 4 °C. Green crystals of 11/11a·CD₂Cl₂ were formed from a CD₂Cl₂ solution of **11** kept at room temperature for 3 d. Suitable single crystals were embedded

in protective perfluoropolyether oil. Data were collected with a Bruker-Nonius KappaCCD diffractometer using Mo-*K*_α radiation (λ = 71.073 pm), and a graphite monochromator. A numerical absorption correction was performed for 3·2CH₃CN. Absorption effects for the other compounds were corrected on a semiempirical basis with the help of multiple scans using either SORT AV^[17a] [5·CH₃OH·(CH₃)₂CO and 0.7511·0.25[Ru(NH₃)(py^{bu}S₄-O₂)]BF₄·CD₂Cl₂] or SADABS^[17b] (4·CH₂Cl₂·0.5*n*-pentane). All structures were solved by direct methods, and full-matrix least-squares refinement was carried out on *F*² using SHELXTL NT 5.1 and NT 6.12.^[18] All non-hydrogen atoms were refined anisotropically. The hydrogen atoms of 11/11a·CD₂Cl₂ were located from a difference Fourier map, while in all other compounds the H atoms were geometrically positioned with isotropic displacement parameters being 1.5-times *U*(eq) of the parent C or N atom. One of the CH₃CN molecules of **3** is disordered, and two alternative sites were refined to 52(2)% (N4, C5, S6) and 48(2)% (N4', C5', S6'). Two alternative sites were refined for one of the *t*Bu groups of **4** to 66(2)% (C55–C57) and 34(2)% (C55'–C57'). In 11a·CD₂Cl₂, the S4 atom is partially oxidized, with the two O atoms having occupancy factors of 25(1)% each. Selected crystallographic parameters and refinement details are summarized in Table 2. Crystallographic data for 4·0.5*n*-pentane have only been deposited with the Cambridge Crystallographic Data Base.^[20]

Acknowledgments

Financial support of these investigations by the Deutsche Forschungsgemeinschaft (SFB 583: Redoxaktive Metallkomplexe) is gratefully acknowledged. We thank Prof. Dr. Horst Kisch for helpful suggestions.

Table 2. Selected crystallographic data for [Ru(CH₃CN)(py^{bu}S₄)]·2CH₃CN (3·2CH₃CN), [Ru(NH₃(py^{bu}S₄)]·CH₂Cl₂·0.5*n*-pentane (4·CH₂Cl₂·0.5*n*-pentane), [Ru(CO)(py^{bu}S₄)]·CH₃OH·(CH₃)₂CO [5·CH₃OH·(CH₃)₂CO], [Ru(NH₃(py^{bu}S₄)]BF₄·CD₂Cl₂ (11·CD₂Cl₂) and [Ru(NH₃(py^{bu}S₄-O₂)]BF₄·CD₂Cl₂ (11a·CD₂Cl₂)

	3·2MeCN	4·CH ₂ Cl ₂ ·0.5 <i>n</i> -pentane	5·MeOH·Me ₂ CO	11·CD ₂ Cl ₂ /11a·CD ₂ Cl ₂
Empirical formula	C ₄₁ H ₅₆ N ₄ RuS ₄	C _{38.5} H ₅₈ Cl ₂ N ₂ RuS ₄	C ₄₀ H ₅₇ NO ₃ RuS ₄	C ₃₆ H ₅₂ BCl ₂ F ₄ N ₂ O _{0.5} RuS ₄
<i>M</i> _r [g/mol]	834.21	849.08	829.18	907.82
Crystal system	monoclinic	triclinic	orthorhombic	monoclinic
Space group	<i>P</i> 2 ₁ / <i>n</i>	<i>P</i> 1	<i>P</i> na2 ₁	<i>P</i> 2 ₁ / <i>n</i>
<i>a</i> [pm]	1757.5(2)	911.2(1)	3241.4(2)	1067.8(2)
<i>b</i> [pm]	1497.9(2)	1307.3(2)	952.54(8)	1400.0(2)
<i>c</i> [pm]	1776.8(1)	1818.8(2)	1320.43(8)	2745.8(3)
α [°]	90	93.775(7)	90.0	90
β [°]	111.92(1)	94.166(7)	90.0	94.826(8)
γ [°]	90	101.679(8)	90.0	90
<i>V</i> [nm ³]	4.3394(8)	2.1089(5)	4.0769(5)	4.0902(8)
<i>Z</i>	4	2	4	4
<i>d</i> _{calcd.} [g/cm ³]	1.277	1.337	1.351	1.474
Temperature [K]	100(2)	100(2)	100(2)	100(2)
μ [mm ^{−1}]	0.586	0.725	0.626	0.767
<i>F</i> (000)	1752	890	1744	1876
Crystal size [mm]	0.17 × 0.15 × 0.06	0.34 × 0.25 × 0.11	0.24 × 0.14 × 0.02	0.25 × 0.22 × 0.10
2 θ range [°]	6.8–50.0	6.6–55.0	6.6–54.0	6.1–54.2
<i>T</i> _{min} / <i>T</i> _{max}	0.914/0.977	0.756/1.000	0.881/0.985	0.838/0.963
Measd. refl.	39123	37179	22814	74469
Indep. refl.	7631	9507	8252	8986
Obsd. refl.	4754	6523	4918	6099
Ref. parameter	495	493	444	625
<i>R</i> 1 [<i>I</i> > 2 σ (<i>I</i>)]	0.0665	0.0488	0.0570	0.0525
<i>wR</i> 2 (all data)	0.1550	0.1110	0.1166	0.1057
$\Delta\rho_{\text{max/min}}$ [Å ³]	1.163/−0.676	0.859/−0.680	0.678/−0.557	0.584/−0.560
Absolute structure parameter ^[19]	—	—	0.01(4)	—

- [1] [1a] J. B. Howard, D. C. Rees, *Chem. Rev.* **1996**, *96*, 2965–2982. [1b] B. K. Burgess, D. J. Lowe, *Chem. Rev.* **1996**, *96*, 2983–3011. [1c] R. R. Eady, *Chem. Rev.* **1996**, *96*, 3013–3030. [1d] R. N. F. Thorneley, D. J. Lowe, *J. Biol. Inorg. Chem.* **1996**, *1*, 576–580. [1e] D. C. Rees, J. B. Howard, *Curr. Opin. Chem. Biol.* **2000**, *4*, 559–566. [1f] O. Einsle, F. A. Tezcan, S. L. A. Andrade, B. Schmid, M. Yoshida, J. B. Howard, D. C. Rees, *Science* **2002**, *297*, 1696–1700.
- [2] [2a] H. Deng, R. Hofmann, *Angew. Chem.* **1993**, *105*, 1125–1128; *Angew. Chem. Int. Ed. Engl.* **1993**, *32*, 1062–1065. [2b] M. D. Fryzuk, S. A. Johnson, *Coord. Chem. Rev.* **2000**, *200–202*, 379–409. [2c] D. Sellmann, A. Fürsattel, J. Sutter, *Coord. Chem. Rev.* **2000**, *200–202*, 545–561.
- [3] [3a] R. A. Henderson, C. J. Leigh, C. J. Pickett, *Adv. Inorg. Chem. Radiochem.* **1983**, *27*, 197–292. [3b] M. Hidai, Y. Mizobe, *Chem. Rev.* **1995**, *95*, 1115–1133. [3c] D. V. Yandulov, R. R. Schrock, *Science* **2003**, *301*, 76–78. [3d] B. A. MacKay, M. D. Fryzuk, *Chem. Rev.* **2004**, *104*, 385–401.
- [4] [4a] Y. Yoshida, T. Adachi, M. Kamanica, T. Ueda, *J. Am. Chem. Soc.* **1988**, *110*, 4872–4873. [4b] R. H. Morris, J. M. Rassner, J. F. Sawyer, M. Shiralian, *J. Am. Chem. Soc.* **1984**, *106*, 3683–3684. [4c] J. Chatt, R. H. Crabtree, J. R. Dilworth, R. L. Richards, *J. Chem. Soc., Dalton Trans.* **1974**, 2358–2362. [4d] J. R. Dilworth, J. Hu, R. H. Thompson, D. L. Hughes, *J. Chem. Soc., Chem. Commun.* **1992**, 551–553; and references cited therein. [4e] M. B. O'Regan, A. H. Liu, W. C. Finck, R. R. Schrock, *J. Am. Chem. Soc.* **1990**, *112*, 4331–4338.
- [5] [5a] D. Sellmann, B. Hautsch, A. Rösler, F. W. Heinemann, *Angew. Chem.* **2001**, *113*, 1553–1555; *Angew. Chem. Int. Ed.* **2001**, *40*, 1505–1508. [5b] D. Sellmann, A. Hille, F. W. Heinemann, M. Moll, A. Rösler, J. Sutter, G. Brehm, M. Reiher, B. A. Hess, S. Schneider, *Inorg. Chim. Acta* **2003**, *348*, 194–198.
- [6] [6a] D. Sellmann, J. Utz, N. Blum, F. W. Heinemann, *Coord. Chem. Rev.* **1999**, *190–192*, 607–627. [6b] D. Sellmann, J. Sutter, *Prog. Inorg. Chem.* **2003**, *52*, 585–681.
- [7] D. Sellmann, R. Prakash, F. W. Heinemann, M. Moll, M. Klimowicz, *Angew. Chem.* **2004**, *116*, 1913–1916; *Angew. Chem. Int. Ed.* **2004**, *43*, 1877–1880.
- [8] [8a] D. Sellmann, J. Utz, F. W. Heinemann, *Inorg. Chem.* **1999**, *38*, 5314–5322. [8b] D. Sellmann, D. Häußinger, T. Gottschalk-Gaudig, F. W. Heinemann, *Z. Naturforsch., Teil B* **2000**, *55*, 723–729. [8c] D. Sellmann, T. Gottschalk-Gaudig, F. W. Heinemann, *Inorg. Chem.* **1998**, *37*, 3982–3988.
- [9] D. Sellmann, T. Gottschalk-Gaudig, D. Häußinger, F. W. Heinemann, B. A. Hess, *Chem. Eur. J.* **2001**, *7*, 2099–2103.
- [10] D. Sellmann, K. Engl, F. W. Heinemann, *Eur. J. Inorg. Chem.* **2000**, 423–429.
- [11] *Recent Advances in Hydride Chemistry* (Eds.: M. Peruzzini, R. Poli), Elsevier, Amsterdam, **2001**, and references cited therein.
- [12] [12a] S. D. Pell, J. N. Armor, *J. Am. Chem. Soc.* **1972**, *94*, 686–687. [12b] S. D. Pell, J. N. Armor, *J. Am. Chem. Soc.* **1973**, *95*, 7625–7633.
- [13] J. D. Buhr, H. Taube, *Inorg. Chem.* **1980**, *19*, 2425–2434.
- [14] [14a] H. M. Koepp, H. Wendt, H. Strehlow, *Z. Elektrochem.* **1960**, *64*, 483–491. [14b] G. Gritzner, J. Kuta, *Pure Appl. Chem.* **1984**, *56*, 461–466.
- [15] A. J. Bard, L. R. Faulkner, *Electrochemical Methods, Fundamentals and Applications*, Wiley, New York, **1980**.
- [16] [16a] D. Sellmann, R. Prakash, F. W. Heinemann, *Eur. J. Inorg. Chem.* **2004**, 1847–1858. [16b] D. Sellmann, R. Prakash, F. Geipel, F. W. Heinemann, *Eur. J. Inorg. Chem.* **2002**, 2138–2346.
- [17] [17a] R. H. Blessing, *Acta Crystallogr., Sect. A* **1995**, *51*, 33–38. [17b] SADABS, Bruker AXS, Inc., Madison, WI, USA, **2002**.
- [18] [18a] SHELXTL NT 5.1, Bruker AXS, Inc., Madison, WI, USA, **1998**. [18b] SHELXTL NT 6.12, Bruker AXS, Inc., Madison, WI, USA, **2002**.
- [19] F. D. Flack, *Acta Crystallogr., Sect. A* **1983**, *39*, 876–881.
- [20] CCDC-238008 (**3**·2CH₃CN), -238009 (**4**·CH₂Cl₂·0.5*n*-pentane), -238012 (**4**·0.5*n*-pentane), -238010 (**5**·CH₃OH·Me₂CO) and -238011 (**11/11a**·CD₂Cl₂) contain the supplementary crystallographic data for this paper. These data can be obtained free of charge at www.ccdc.cam.ac.uk/conts/retrieving.html [or from the Cambridge Crystallographic Data Centre, 12 Union Road, Cambridge CB2 1EZ, UK; Fax: + 44-1223-336-033; E-mail: deposit@ccdc.cam.ac.uk].

Received May 7, 2004

Early View Article

Published Online September 7, 2004